The EMBO Journal Vol. 20 No. 1 & 2 pp. 77–81, 2001

The projection structure of EmrE, a proton-linked multidrug transporter from *Escherichia coli*, at 7 Å resolution

Christopher G.Tate[1,2], Edmund R.S.Kunji[1,3], Mario Lebendiker[4] and Shimon Schuldiner[4]

[1]MRC Laboratory of Molecular Biology, Hills Road, Cambridge CB2 2QH, [3]MRC Dunn Human Nutrition Unit, Hills Road, Cambridge CB2 2XY, UK and [4]Institute of Life Sciences, Givat Ram, Hebrew University, Jerusalem 91904, Israel

[2]Corresponding author
e-mail: cgt@mrc-lmb.cam.ac.uk

EmrE belongs to a family of eubacterial multidrug transporters that confer resistance to a wide variety of toxins by coupling the influx of protons to toxin extrusion. EmrE was purified and crystallized in two dimensions by reconstitution with dimyristoylphosphatidylcholine into lipid bilayers. Images of frozen hydrated crystals were collected by cryo-electron microscopy and a projection structure of EmrE was calculated to 7 Å resolution. The projection map shows an asymmetric EmrE dimer with overall dimensions ~31 × 40 Å, comprising an arc of highly tilted helices separating two helices nearly perpendicular to the membrane from another two helices, one tilted and the other nearly perpendicular. There is no obvious 2-fold symmetry axis perpendicular to the membrane within the dimer, suggesting that the monomers may have different structures in the functional unit.

Keywords: ion-coupled transport/membrane proteins/multidrug resistance/structure

Introduction

Bacteria have naturally developed a wide variety of systems that are capable of extruding toxic compounds out of the cell, which has given rise to the multidrug resistance phenotype that is currently a widespread problem in medicine (Nikaido, 1994). Determining the structure of multidrug transporters will give a better understanding of the mechanism of multidrug efflux and may lead to therapeutic strategies to counter the multidrug resistance phenomenon. EmrE belongs to the family of the smallest known multidrug transporters, the small multidrug resistance (SMR) family (Paulsen *et al*., 1996), and is thus an ideal candidate for structure–function studies (Schuldiner *et al*., 1997). Members of the SMR family characteristically contain between 100 and 120 amino acid residues that are predicted to form four transmembrane regions, but their orientation in the membrane has not yet been determined. Many eubacterial genomes sequenced so far contain SMR transporters, often with multiple types in a single genome, but their physiological substrates remain, for the most part, undetermined. The most striking feature of EmrE is that it is capable of transporting substrates of widely varying structure, provided that overall the compound is highly hydrophobic and carries a positive charge (reviewed in Schuldiner *et al*., 1996). EmrE couples the extrusion of toxins to the influx of protons down their electrochemical gradient, with probably two or more protons transported per toxin molecule (Yerushalmi *et al*., 1995; Yerushalmi and Schuldiner, 2000a).

EmrE contains only 110 amino acid residues, which from the hydropathic profile are predicted to form four transmembrane regions (Yerushalmi *et al*., 1995). This prediction is supported experimentally by Fourier transform infrared spectroscopy (FTIR) of EmrE in lipid bilayers and in organic solvents, which reveals that the secondary structure is 78–80% α-helical (Arkin *et al*., 1996). High-resolution heteronuclear NMR of EmrE in organic solvent also supports the four-helix model (Schwaiger *et al*., 1998). However, given its small size and that the majority of bacterial transporters contain 12 transmembrane domains, it seemed unlikely that EmrE would function as a monomer. Negative dominance studies suggested that EmrE was an oligomer (Yerushalmi *et al*., 1996), although the data were not sufficient to differentiate clearly between a dimeric or trimeric model. Radiolabelled substrate binding to purified EmrE showed one inhibitor bound per three molecules of EmrE (Muth and Schuldiner, 2000; Yerushalmi and Schuldiner, 2000b), supporting the evidence for a trimer. However, the possibility that EmrE functions as a dimer or a tetramer was not ruled out (Muth and Schuldiner, 2000). We have obtained two-dimensional crystals of EmrE and calculated a projection structure showing that EmrE is a dimer, thus providing a solid foundation for future studies on the molecular mechanism of toxin extrusion.

Results and discussion

EmrE with a His_6 tag at the C-terminus was expressed in *Escherichia coli* and purified in dodecylmaltoside (DDM) as previously described (Muth and Schuldiner, 2000). Dialysis of the concentrated EmrE for 10–14 days, in the absence of any added lipid, yielded poorly ordered crystals with a *c*222 symmetry (cell dimensions 73 × 163 Å; results not shown). The *c*222 crystals were only a small percentage of the total vesicles present, the other vesicles being large and extensively folded, suggesting that the purified EmrE contained substantial amounts of *E.coli* lipid. The inclusion of 400 mM NaCl during purification, or the addition of an ion-exchange step, seemed to reduce the amount of lipid co-purifying with EmrE as assessed by a glycolipid analysis using silver-stained tricine–SDS–polyacrylamide gels (Lesse *et al*., 1990). Crystallization trials then yielded conditions that gave numerous crystals, which appeared as tubes and triangular vesicles by electron microscopy of negatively stained samples

(Figure 1). All the crystals were of $p222_1$ symmetry (cell dimensions 84 × 74 Å) with the flattened tubes being the best ordered of the crystal shapes. Images of negatively stained crystals contained two lattices from the two membrane layers in the flattened tube, and the orientation between the lattices was variable. For the collection of high-resolution data, frozen hydrated crystals were examined by cryo-electron microscopy. Only a single lattice was observed in images of crystals in ice. Single untilted images contained data after processing to at least 7 Å resolution, with some data to 6 Å (Figure 2). The eight best untilted images were processed and merged to yield an electron density projection map (Figure 3) with good phase residuals to 7 Å (Table I). A comparison of the crystal packing in the *c*222 crystals (not shown) and $p222_1$ crystals shows that the major crystal contacts between the asymmetric units (Figure 3B) are conserved. The only crystal contact that is not conserved between the two crystal forms is along the 2-fold screw axis bisecting the unit cell as defined in Figure 3A; in the *c*222 crystal, the crystallographic dimer is translated along this screw axis by ~37 Å.

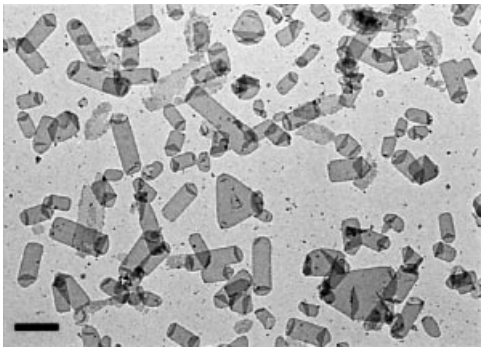

Fig. 1. Electron micrograph of EmrE crystals stained with 1% phosphotungstate pH 7. The scale bar corresponds to 1 μm.

The projection density shows an asymmetric structure of dimensions ~31 × 40 Å that is closely associated with the neighbouring structural unit to form what is most likely

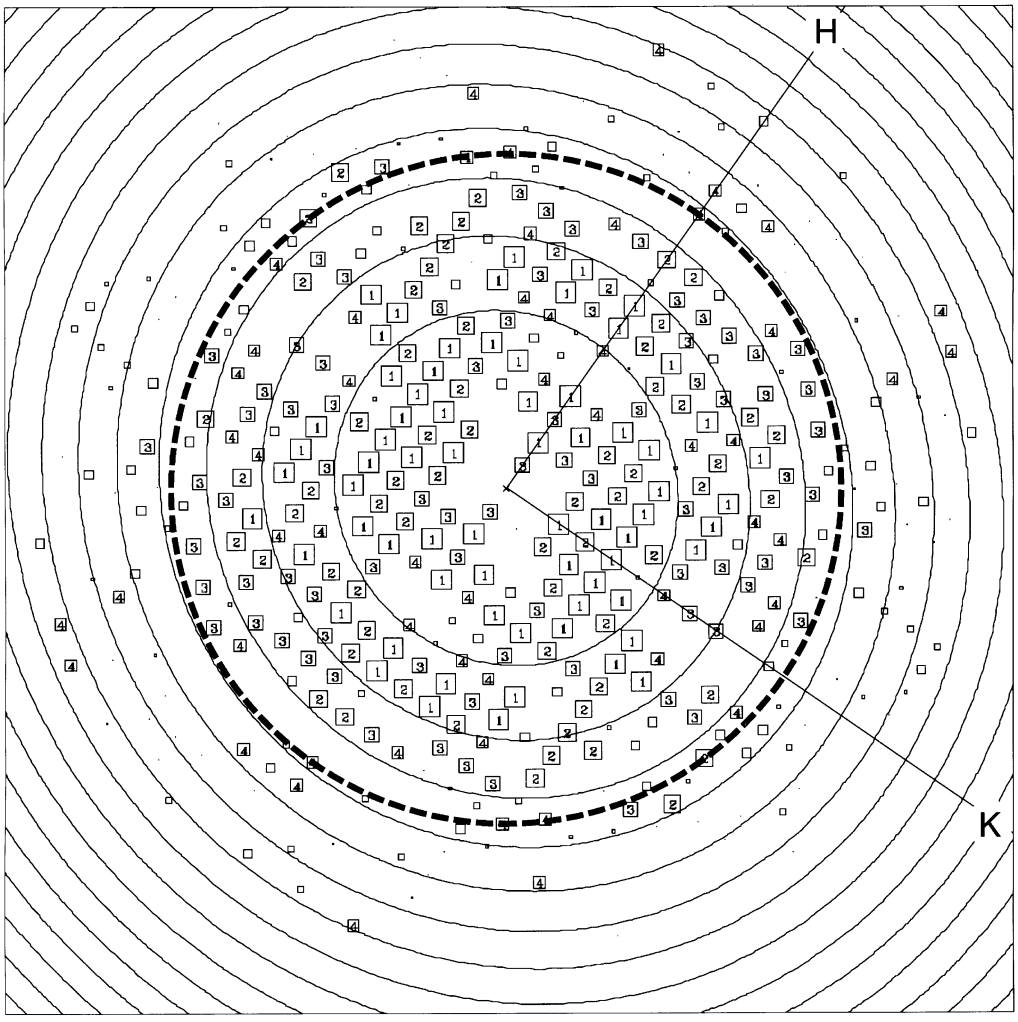

Fig. 2. Calculated Fourier components of an EmrE image after correction for lattice distortions and removal of background noise. Boxes represent the position of each diffraction spot. The IQ value represents the signal to noise ratio of the amplitude for each spot; strong spots with IQ values from 1 to 4 are represented by a number in a box and weak spots with IQ values from 5 to 8 are represented by progressively smaller boxes. An IQ value of 1 means that the signal is >7 times greater than background after correction for the background noise, while IQ 7 is equal to background after correction. The 7 Å resolution limit is depicted by a circle of dashes. The concentric circles represent the zero of the contrast transfer function.

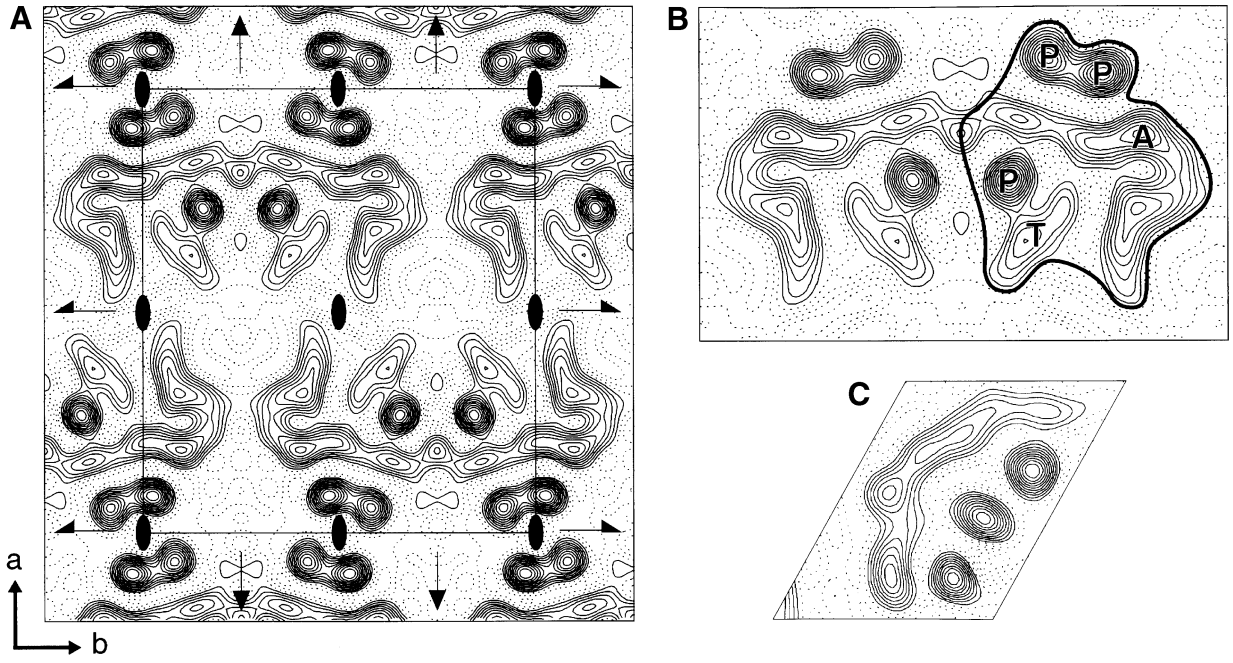

Fig. 3. Projection map of EmrE at 7.0 Å resolution. (**A**) The electron density map was calculated from eight merged images with $p222_1$ symmetry applied. A single unit cell is shown with its symmetry elements: 2-fold axes perpendicular to the membrane plane (ovals), 2-fold screw axes (half arrows) parallel to *b* and 2-fold axes in the plane of the membrane (arrows) parallel to *a*. The *a* and *b* axes are defined in the bottom left corner. Statistics for the map are shown in Table I. (**B**) A crystallographic dimer is shown, with the asymmetric structure outlined. Note that the asymmetric units are related by a 2-fold axis in the plane of the membrane, i.e. they have different orientations in the membrane. The interpretation of the electron density features made in the main text are as follows: P, an α-helix nearly perpendicular to the membrane plane; T, probably a single α-helix tilted with respect to the membrane normal; A, an arc of probably four tilted α-helices. (**C**) The projection map of bacteriorhodopsin at 7 Å resolution has been scaled exactly to (B), allowing a direct comparison of sizes.

Table I. Electron crystallographic data

Plane group symmetry	$p222_1$
Unit cell dimensions	a = 84.44 ± 0.62 Å b = 73.85 ± 0.08 Å γ = 90.0 ± 0.7°
No. of images	8
Range of defocus	2260–9234 Å
No. of unique reflections to 7 Å	107
Total no. of observations to 7 Å	1384
Overall phase residual to 7 Å (random = 90°)	27.54°
Temperature factor B_{xy} (restores high-resolution contrast by correction for in-plane amplitude fall-off)	339 ± 11

Resolution range (Å)	No. of unique reflections	Phase residual (random = 45°)
200–12.0	45	11.9°
12.0–9.5	22	11.8°
9.5–8.2	20	19.0°
8.2–6.9	30	16.7°
6.9–6.3	20	30.7°
6.3–5.7	31	38.1°

a crystallographic dimer (Figure 3B). The 2-fold axis in the plane of the membrane relates the two asymmetric structures to each other, i.e. the molecules in each unit would have opposite orientations in the membrane. Whether the crystallographic dimer represents the functional EmrE unit *in vivo* remains to be explored. Each asymmetric structure is composed of three well-defined circles of electron density, a continuous band of electron density extending for ~55 Å and a short cylinder of density adjacent to one of the circles. These features are similar to those found in a projection map at the same resolution of bacteriorhodopsin (bR; Figure 3C), whose atomic structure is known (Grigorieff *et al*., 1996), which therefore allows an interpretation of the EmrE projection map to be made. The three circles of density probably represent α-helices that are nearly perpendicular to the membrane. The 55 Å band of electron density is of similar dimensions to the 50 Å-long band of electron density that corresponds to four tilted helices in the bR structure, the small cylinder of density probably corresponding to a single tilted helix. The slight difference between the length of the four tilted helices in EmrE and bR is consistent with an overall greater tilt of helices in EmrE, predicted to be 27° from FTIR data (Arkin *et al*., 1996), and the average tilt of bR helices, which is 16° as determined from the atomic resolution structure (Grigorieff *et al*., 1996). This interpretation of the electron density map suggests that there are eight α-helices in the EmrE asymmetric unit. The overall dimensions of EmrE (~31 × 40 Å) are also considerably smaller than the dimensions of NhaA, a 12-helix transporter (~38 × 48 Å; Williams *et al*., 1999), suggesting that a 12-helix model for EmrE based on the projection data is unlikely.

How does the amino acid sequence of EmrE relate to the projection structure? EmrE has 110 amino acids that are predicted to contain four hydrophobic α-helices, this

interpretation being supported by FTIR and NMR data (Arkin *et al*., 1996; Schwaiger *et al*., 1998). The suggestion of eight α-helices per asymmetric unit in the projection map implies that EmrE is a dimer, assuming that the asymmetric unit is the functional EmrE oligomer. This assumption seems reasonable given that EmrE exists as a functional oligomer in the detergent used for purification and crystallization (Muth and Schuldiner, 2000; Yerushalmi and Schuldiner, 2000b), although it has been difficult to determine the precise number of subunits per oligomer. Negative dominance experiments suggested that EmrE was a dimer or a trimer (Yerushalmi *et al*., 1996), and recent binding data seemed to lend more weight to the argument for a trimer (Muth and Schuldiner, 2000; Yerushalmi and Schuldiner, 2000b). However, the latter experiments were critically dependent on accurate determination of the absolute EmrE concentration and on having a 100% active protein preparation, both of which are notoriously difficult to obtain for integral membrane proteins. The projection map is firm evidence in favour of an EmrE dimer. Although unlikely, we cannot rule out the possibility that the functional unit is a tetramer formed from two dimers.

The deduction that EmrE is a dimer naturally raises the question of how the monomers are related to each other, because there is no obvious 2-fold symmetry axis perpendicular to the membrane as may be expected. Certainly, structures of other integral membrane proteins that are oligomeric have clear pseudo- or crystallographic symmetry axes perpendicular to the membrane, relating monomers to each other (see for example, Hebert *et al*., 1995; Doyle *et al*., 1998; Unger *et al*., 1999). At this stage it cannot be ruled out that there is a highly tilted 2-fold axis in the EmrE dimer, the tilt making it very difficult to see. Considering the proposed arrangement of helices, this does not seem likely. A more intriguing possibility is that the two monomers do not have identical structures, despite having the same amino acid sequence. This phenomenon has been observed previously in the structure of soluble protein dimers (Carrell *et al*., 1994; Hirsch *et al*., 1999). Two different structures for each EmrE monomer introduce a potential non-equivalence in structural environment for the Glu14 residues that are instrumental for both toxin translocation and the transport of two protons (Muth and Schuldiner, 2000). This raises exciting questions for the mechanism of transport and the associated conformational changes; in particular, is the asymmetry maintained through the transport cycle, or is there an oscillation of the monomers between two structurally distinct conformations? Further insights will be possible from a three-dimensional structure determination of EmrE that is in progress.

Materials and methods

Overexpression and purification of EmrE were performed using the EmrE-His construct and the methods described (Muth and Schuldiner, 2000), except that 400 mM NaCl was used in all the buffers. An additional anion-exchange step performed at pH 8.0 was also found to be effective in the removal of glycolipids. After purification, EmrE was concentrated to 1 mg/ml using Centricons (Amicon) with a molecular weight cut-off of 10 000 Da. Two-dimensional crystallization was performed by dialysis of 100–200 µl samples in Slide-a-lyzers (Pierce) containing a final EmrE concentration of 0.5 mg/ml, as estimated using a protein assay with bovine serum albumin as standard (Schaffner and Weissmann, 1973). Prior to dialysis, CHAPS (0.25–1% final concentration) and dimyristoylphosphatidylcholine [lipid to protein ratio (w/w) of between 0.1 and 0.4] were added to EmrE, which was then dialysed against 20 mM sodium phosphate pH 7.0, 50 mM NaCl, 2 mM $MgCl_2$, 1 mM EDTA, 20 mM sodium azide. The buffer was changed daily. Crystals appeared 10–14 days later.

Screening of crystals was performed on a Phillips CM12 electron microscope with samples stained with 1% phosphotungstate pH 7. Cryo-electron microscopy of frozen hydrated EmrE crystals was performed on a 200 keV Hitachi HF2000 microscope with a cold field emission gun, using a Gatan 626 cryo-stage cooled by liquid nitrogen. Images were collected with flood beam illumination at a magnification of 50 000 with film exposure times of 1.0–2.5 s under standard low dose conditions (10–15 $e^-/Å^2$). Films were screened for crystalline areas initially by optical diffraction, the best images were then digitized using a Zeiss SCAI scanner with a 7 µm step size. All image processing to correct for lattice distortions, astigmatism and the contrast transfer function were performed using the MRC image processing programs (Crowther *et al*., 1996) and followed earlier protocols (Havelka *et al*., 1993, 1995). Recent improvements in the software used included the calculation of defocus and astigmatism values by CTFFIND2 (Grigorieff, 1998) and the determination of the phase origin and plane group symmetry by ALLSPACE (Valpuesta *et al*., 1994). After origin refinement and merging of the CTF-corrected data, the image amplitudes were scaled to diffraction data of bR and projection maps were calculated (Havelka *et al*., 1993, 1995).

Acknowledgements

We are extremely grateful for the help and advice of R.Henderson throughout this project. This work was supported by the Medical Research Council, and by grants NS16708 from the National Institutes of Health and 463/00 from The Israel Science Foundation.

References

Arkin,I.T., Russ,W.P., Lebendiker,M. and Schuldiner,S. (1996) Determining the secondary structure and orientation of EmrE, a multidrug transporter, indicates a transmembrane four-helix bundle. *Biochemistry*, **35**, 7233–7238.

Carrell,R.W., Stein,P.E., Fermi,G. and Wardell,M.R. (1994) Biological implications of a 3 Å structure of dimeric antithrombin. *Structure*, **2**, 257–270.

Crowther,R.A., Henderson,R. and Smith,J.M. (1996) MRC image processing programs. *J. Struct. Biol.*, **116**, 9–16.

Doyle,D.A., Morais Cabral,J., Pfuetzner,R.A., Kuo,A., Gulbis,J.M., Cohen,S.L., Chait,B.T. and MacKinnon,R. (1998) The structure of the potassium channel: molecular basis of K^+ conduction and selectivity. *Science*, **280**, 69–77.

Grigorieff,N. (1998) Three-dimensional structure of bovine NADH:ubiquinone oxidoreductase (complex I) at 22 Å in ice. *J. Mol. Biol.*, **277**, 1033–1046.

Grigorieff,N., Ceska,T.A., Downing,K.H., Baldwin,J.M. and Henderson,R. (1996) Electron-crystallographic refinement of the structure of bacteriorhodopsin. *J. Mol. Biol.*, **259**, 393–421.

Havelka,W.A., Henderson,R., Heymann,J.A. and Oesterhelt,D. (1993) Projection structure of halorhodopsin from *Halobacterium halobium* at 6 Å resolution obtained by electron cryo-microscopy. *J. Mol. Biol.*, **234**, 837–846.

Havelka,W.A., Henderson,R. and Oesterhelt,D. (1995) Three-dimensional structure of halorhodopsin at 7 Å resolution. *J. Mol. Biol.*, **247**, 726–738.

Hebert,H., Schmidt-Krey,I. and Morgenstern,R. (1995) The projection structure of microsomal glutathione transferase. *EMBO J.*, **14**, 3864–3869.

Hirsch,J.A., Schubert,C., Gurevich,V.V. and Sigler,P.B. (1999) The 2.8 Å crystal structure of visual arrestin: a model for arrestin's regulation. *Cell*, **97**, 257–269.

Lesse,A.J., Campagnari,A.A., Bittner,W.E. and Apicella,M.A. (1990) Increased resolution of lipopolysaccharides and lipooligosaccharides utilizing tricine–sodium dodecyl sulfate–polyacrylamide gel electrophoresis. *J. Immunol. Methods*, **126**, 109–117.

Muth,T.R. and Schuldiner,S. (2000) A membrane-embedded glutamate

is required for ligand binding to the multidrug transporter EmrE. *EMBO J.*, **19**, 234–240.

Nikaido,H. (1994) Prevention of drug access to bacterial targets: permeability barriers and active efflux. *Science*, **264**, 382–388.

Paulsen,I.T., Skurray,R., Tam,R., Saier,M., Turner,R., Weiner,J., Goldberg,E. and Grinius,L. (1996) The SMR family: a novel family of multidrug efflux proteins involved with the efflux of lipophilic drugs. *Mol. Microbiol.*, **19**, 1167–1175.

Schaffner,W. and Weissmann,C. (1973) A rapid, sensitive and specific method for the determination of protein in dilute solution. *Anal. Biochem.*, **56**, 502–514.

Schuldiner,S., Lebendiker,M., Mordoch,S., Yelin,R. and Yerushalmi,H. (1996) From multidrug resistance to vesicular neurotransmitter transport. In Konings,W.N., Kaback,H.R. and Lolkema,J.S. (eds), *Transport Processes in Membranes.* Elsevier, Amsterdam, The Netherlands.

Schuldiner,S., Lebendiker,M. and Yerushalmi,H. (1997) EmrE, the smallest ion-coupled transporter, provides a unique paradigm for structure–function studies. *J. Exp. Biol.*, **200**, 335–341.

Schwaiger,M., Lebendiker,M., Yerushalmi,H., Coles,M., Groger,A., Schwarz,C., Schuldiner,S. and Kessler,H. (1998) NMR investigation of the multidrug transporter EmrE, an integral membrane protein. *Eur. J. Biochem.*, **254**, 610–619.

Unger,V.M., Kumar,N.M., Gilula,N.B. and Yeager,M. (1999) Three-dimensional structure of a recombinant gap junction membrane channel. *Science*, **283**, 1176–1180.

Valpuesta,J.M., Carrascosa,J.L. and Henderson,R. (1994) Analysis of electron microscope images and electron diffraction patterns of thin crystals of ϕ29 connectors in ice. *J. Mol. Biol.*, **240**, 281–287.

Williams,K.A., Geldmacher-Kaufer,U., Padan,E., Schuldiner,S. and Kuhlbrandt,W. (1999) Projection structure of NhaA, a secondary transporter from *Escherichia coli*, at 4.0 Å resolution. *EMBO J.*, **18**, 3558–3563.

Yerushalmi,H. and Schuldiner,S. (2000a) A common binding site for substrates and protons in EmrE, an ion-coupled multidrug transporter. *FEBS Lett.*, **476**, 93–97.

Yerushalmi,H. and Schuldiner,S. (2000b) An essential glutamyl residue in EmrE, a multidrug antiporter from *Escherichia coli*. *J. Biol. Chem.*, **275**, 5264–5269.

Yerushalmi,H., Lebendiker,M. and Schuldiner,S. (1995) EmrE, an *Escherichia coli* 12-kDa multidrug transporter, exchanges toxic cations and H^+ and is soluble in organic solvents. *J. Biol. Chem.*, **270**, 6856–6863.

Yerushalmi,H., Lebendiker,M. and Schuldiner,S. (1996) Negative dominance studies demonstrate the oligomeric structure of EmrE, a multidrug antiporter from *Escherichia coli*. *J. Biol. Chem.*, **271**, 31044–31048.

Received October 16, 2000; revised and accepted November 7, 2000